Human Molecular Genetics, 2011, Vol. 20, No. 9 ***1763–1775***
doi:10.1093/hmg/ddr059
Advance Access published on February 11, 2011

Zebrafish Fukutin family proteins link the unfolded protein response with dystroglycanopathies

Yung-Yao Lin[1], Richard J. White[1], Silvia Torelli[2], Sebahattin Cirak[2], Francesco Muntoni[2] and Derek L. Stemple[1,*]

[1]Wellcome Trust Sanger Institute, Wellcome Trust Genome Campus, Hinxton, Cambridge CB10 1SA, UK and [2]Dubowitz Neuromuscular Centre, Institute of Child Health, University College London, London, UK

Received December 3, 2010; Revised and Accepted February 6, 2011

Allelic mutations in putative glycosyltransferase genes, *fukutin* and *fukutin-related protein (fkrp)*, lead to a wide range of muscular dystrophies associated with hypoglycosylation of α-dystroglycan, commonly referred to as dystroglycanopathies. Defective glycosylation affecting dystroglycan–ligand interactions is considered to underlie the disease pathogenesis. We have modelled dystroglycanopathies in zebrafish using a novel loss-of-function *dystroglycan* allele and by inhibition of Fukutin family protein activities. We show that muscle pathology in embryos lacking Fukutin or FKRP is different from loss of dystroglycan. In addition to hypoglycosylated α-dystroglycan, knockdown of Fukutin or FKRP leads to a notochord defect and a perturbation of laminin expression before muscle degeneration. These are a consequence of endoplasmic reticulum stress and activation of the unfolded protein response (UPR), preceding loss of dystroglycan–ligand interactions. Together, our results suggest that Fukutin family proteins may play important roles in protein secretion and that the UPR may contribute to the phenotypic spectrum of some dystroglycanopathies in humans.

INTRODUCTION

Congenital muscular dystrophies (CMD) are a heterogeneous group of autosomal recessive hereditary diseases affecting infants and representing in some instances severe allelic variants of gene defects that more commonly cause mild forms of limb girdle muscular dystrophies (LGMD) with onset in adolescence or adult life. Approximately 20–30% of classical CMD cases are due to absence of laminin α2 isoform, a subunit of laminin heterotrimers which are essential components of the basement membrane (1–3). This condition, also known as CMD type 1A (MDC1A; OMIM 607855), is a severe CMD variant characterized by laminin α2 deficiency and early onset of progressive muscle degeneration associated with brain white matter hypodensity (4). Rare milder allelic mutations are associated with partial laminin α2 reduction, resembling a late onset of LGMD variant (5–8).

Several other forms of CMD are not primarily caused by laminin α2 deficiency but by mutations in known or putative glycosyltransferase genes, associated with hypoglycosylation of α-dystroglycan. Interestingly, allelic mutations in each of these genes can result in a wide spectrum of clinical severity, ranging from the most severe congenital onset of muscle weakness with structural brain and/or eye abnormalities, such as Walker–Warburg syndrome (WWS; OMIM 236670), muscle–eye–brain disease (MEB; OMIM 253280), Fukuyama-type CMD (FCMD; OMIM 253800) and CMD-type 1D (MDC1D; OMIM 608840), to a milder form without brain involvement, such as CMD-type 1C (MDC1C; OMIM 606612), and the mildest form characterized by late onset of muscle weakness in adulthood without brain involvement, such as LGMD2I (OMIM 607155) (9,10). All these muscular dystrophy variants associated with hypoglycosylation of α-dystroglycan are commonly referred to as secondary dystroglycanopathies.

Dystroglycan is a central component of the dystrophin-associated glycoprotein complex (DGC), providing a mechanical linkage between subsarcolemmal proteins and basement membrane components through its non-covalently connected α and β subunits (11,12). β-dystroglycan is a

*To whom correspondence should be addressed. Tel: +44 1223496857; Fax: +44 1223494919; Email: ds4@sanger.ac.uk

transmembrane protein in the sarcolemma with α-dystroglycan tightly associated at the extracellular periphery. The C-terminal cytoplasmic tail of β-dystroglycan interacts with dystrophin which binds to the actin cytoskeleton (11). α-dystroglycan acts as a receptor of several extracellular ligands, such as laminins, agrin and perlecan in muscle (11,13–16) and neurexin and pikachurin in the brain and retina, respectively (17,18). The molecular mass of α-dystroglycan varies from 100 to 156 kDa in different tissues as a result of intensive *O*-linked sugar modifications in its mucin domain. It is thought that the tissue-specific *O*-glycosylation within the mucin domain of α-dystroglycan mediates the receptor-ligand binding activities (19). In addition, hypoglycosylation of α-dystroglycan in FCMD, MEB, WWS and MDC1D patients has been associated with disrupted binding activities for its ligands, such as laminins, neurexin or agrin (20–22).

Structural analyses uncovered *O*-mannosyl-type oligosaccharides on functional α-dystroglycan in mammals, including a phosphorylated *O*-mannosyl glycan required for laminin binding (23–26). To date, identified mutations associated with dystroglycanopathies affect genes encoding known or putative glycosyltransferases: protein *O*-mannosyl transferase 1 and 2 (POMT1 and POMT2) (27,28), protein *O*-mannose β1,2-*N*-acetylglucosaminyltransferase 1 (POMGnT1) (29), Fukutin (FKTN) (30), Fukutin-related protein (FKRP) (31) and acetylglucosaminyltransferase-like protein (LARGE) (21,32). Among these, POMT1 and POMT2 form a functional hetero-complex to catalyse the transfer of a mannosyl residue from dolichyl phosphate mannose (Dol-P-Man) to serine or threonine residues of α-dystroglycan (33). Subsequently, POMGnT1 adds an *N*-acetylglucosaminyl residue to the mannose group (29). Notably, deficiency of Dol-P-Man synthase subunit 3 affects both *N*-glycosylation of a number of proteins and *O*-mannosylation of α-dystroglycan, bridging two separate entities of genetic glycosylation disorders (34). The enzymatic activities of Fukutin, FKRP and LARGE still remain to be demonstrated, although LARGE was shown to mediate a post-phosphoryl modification of the phosphorylated *O*-linked mannose, on which the laminin-binding moiety is present (26). While the specific modification critical for laminin-binding remains unknown, less is clear with regard to the wide spectrum of clinical severity in dystroglycanopathies.

Here we model dystroglycanopathies in zebrafish using a novel loss-of-function *dystroglycan* allele and by inhibition of Fukutin or FKRP protein activities. We show that muscle pathology in zebrafish embryos lacking Fukutin or FKRP is different from the loss of dystroglycan. Apart from hypoglycosylated α-dystroglycan, removing Fukutin or FKRP causes notochord differentiation defects and perturbs expression of laminins. Our results imply that Fukutin and FKRP may affect protein secretion beyond glycosylation of α-dystroglycan. We show that knockdown of Fukutin or FKRP leads to endoplasmic reticulum (ER) stress and activation of the unfolded protein response (UPR), preceding disruption of dystroglycan–ligand interactions in muscle. We discuss how the UPR may contribute to the wide spectrum of clinical severity in some forms of dystroglycanopathies in humans.

RESULTS

Loss of dystroglycan disrupts dystrophin but not laminin localization

To model dystroglycanopathies in zebrafish, we characterized a novel *dystroglycan* nonsense mutation allele (*dag1*^{hu3072}), obtained from the Sanger Institute Zebrafish Mutation Resource (35,36). This allele carries a C1568T change, which causes a premature termination of translation (R398 > Stop) within the mucin domain of α-dystroglycan (Fig. 1A and D). Genotype–phenotype analysis identifies *dag1*^{hu3072} as a recessive allele. *dag1* −/− embryos consistently display severe muscular dystrophy that becomes fully penetrant by 48 h post fertilization (hpf), whereas the skeletal muscle of siblings remains unaffected (Fig. 1B and C). To further confirm that the mutation is associated with the dystrophic phenotype, we show that endogenous dystroglycan is neither detected by western blot analysis, nor by immunostaining with α- or β-dystroglycan-specific antibodies in homozygous mutant embryos (Fig. 1E and L), demonstrating that *dag1*^{hu3072} is a complete loss-of-function allele.

Both myogenesis and myofibrillogenesis appear to be unaffected in *dag1* −/− embryos (data not shown). By labelling filamentous-actin (F-actin), we find that the cause of the dystrophic phenotype in the absence of dystroglycan is due to detachment and retraction of muscle fibres from the vertical myosepta, first occurring in the superficial layer of slow muscle, subsequently followed by the deeper layer of fast muscle (Fig. 1G and H). In addition, the onset of dystrophic muscle pathology in *dag1* −/− embryos may occur as early as 36 hpf, shortly after the elongation and fusion of myofibres (data not shown). The muscle pathology of *dag1* −/− embryos is similar to that of *sapje/dystrophin* (*sap/dmd*) and *candyfloss/laminin α2* (*caf/lama2*) −/− embryos (37,38), which led us to investigate sarcolemma integrity using Evans Blue Dye (EBD) and cell death using Acridine Orange. Similar to *sap/dmd* and *caf/lama2* −/− embryos, detached muscle fibres eventually undergo cell death in *dag1* −/− embryos (Supplementary Material, Fig. S4). Unlike *sap/dmd* embryos, we find no evidence for muscle fibres of *dag1* −/− embryos infiltrated by EBD before detachment. Nevertheless, retracted muscle fibres of *dag1* embryos do uptake EBD, in contrast to what is found in *caf/lama2* −/− embryos (Fig. 1F). Together, these results suggest that muscle fibre detachment occurs before disruption of sarcolemma integrity in *dag1* −/− embryos.

To distinguish whether muscle fibre detachment occurs within the basement membrane or at the sarcolemma in *dag1* −/− embryos, we assessed the immunoreactivity of DGC components at the vertical myoseptum, where dystroglycan extracellularly interacts with laminins and intracellularly binds to dystrophin. Here we show that the dystrophic muscle pathology of *dag1* −/− embryos is highly correlated with the loss of dystrophin localization at the vertical myoseptum. In addition, residual dystrophin remains at the free ends of detached muscle fibres (arrows, Fig. 1I and J). Although hypoglycosylation of α-dystroglycan leads to reduced dystroglycan–laminin-binding activity *in vitro* (22), we show that a complete absence of dystroglycan does not give rise to loss of laminin-1 (α1β1γ1) localization (Fig. 1K and L), nor morphological phenotypes resembling shortened zebrafish *laminin* mutants (39) (Fig. 1B

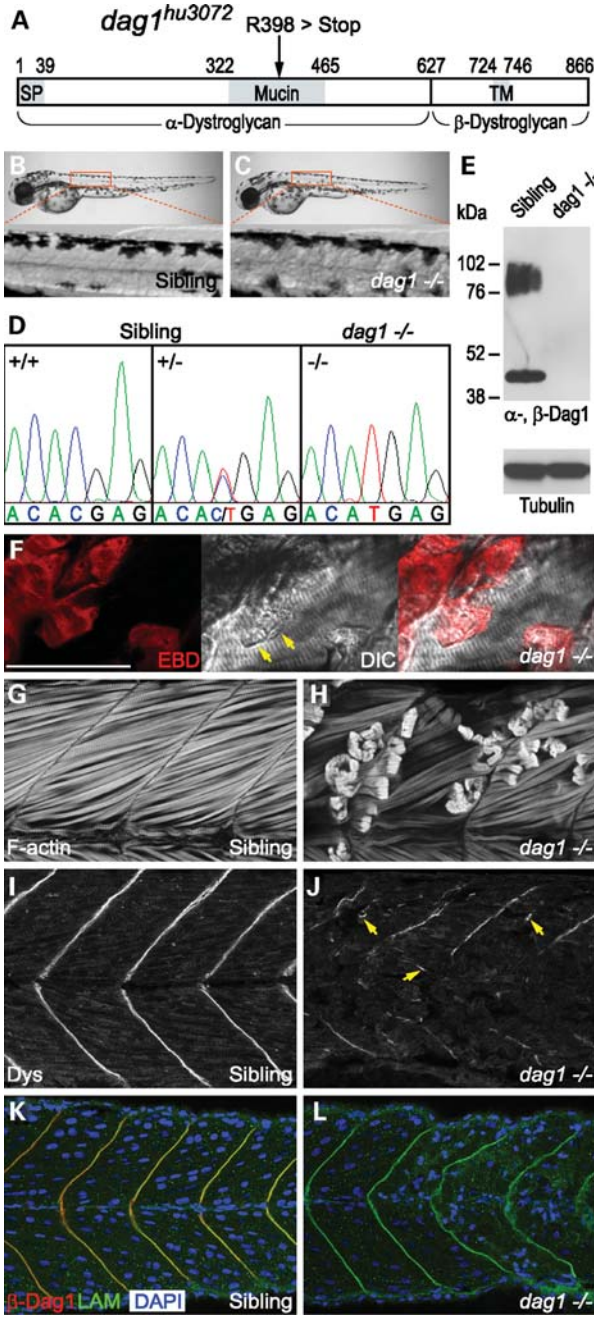

Figure 1. A novel *dystroglycan* nonsense mutation allele elicits severe muscular dystrophy. (**A**) A schematic drawing indicates the position of the mutation (R398>Stop) within the mucin domain of dystroglycan (*dag1*^{hu3072}). SP, signal peptide. TM, transmembrane domain. (**B** and **C**) Dystrophic muscle pathology becomes apparent by 48 hpf, comparing sibling and homozygous mutant embryos. (**D**) Lesions in the muscle are consistently associated with *dag1* −/− embryos. (**E**) Western blot analysis of glycoproteins enriched by WGA shows glycosylated α-Dag1 (IIH6; 76–102 kDa) and β-Dag1 (43 kDa) in the sibling, but not *dag1* −/− embryos (120 hpf). Equivalent protein loading is demonstrated by detection of tubulin. (**F**) Damaged muscle fibres (arrows) and lesions in *dag1* embryos are infiltrated by EBD (red). (**G** and **H**) F-actin labelled by phalloidin showing intact and retracted muscle fibres. (**I** and **J**) A complete absence of dystroglycan leads to dislocated dystrophin associated with free ends of broken muscle fibres (arrows), despite residual dystrophin detected at myoseptum. (**K** and **L**) Laminin-1 (green) localization remains intact at the myoseptum in the *dag1* −/− background, where β-Dag1 (red) is not detected and aberrant morphology of nuclei is associated with dystrophic muscle (blue). (F–L) 48 hpf embryos. Bar, 50 μm.

and C). Due to the onset of muscular dystrophy, however, the shapes of vertical myosepta become distorted in *dag1* −/− embryos (Fig. 1K and L). In brief, the absence of dystroglycan leading to dislocated dystrophin reflects the muscle pathology of *dag1* −/− embryos, in which muscle fibre detachment first occurs within the basement membrane, followed by disruption of sarcolemma integrity.

Muscle pathology in Fukutin or FKRP morpholino oligonucleotide-injected embryos is distinct from dystroglycan mutants

To study the pathogenesis of dystroglycanopathies due to knockdown of Fukutin or FKRP function, we inhibited zebrafish Fukutin family protein activities using low-to-high doses of antisense morpholino oligonucleotides (MOs) (Fig. 2A and D). The specificity of *fukutin* MO was demonstrated by reverse transcription polymerase chain reaction (RT–PCR) and sequencing of the aberrantly spliced transcript (Fig. 2B). *fkrp* MO specifically inhibited the expression of the recombinant FKRP–enhanced green fluorescent protein (EGFP) protein in a concentration-dependent manner (Fig. 2E). The phenotypic severity of *fukutin* or *fkrp* MO-injected embryos is also dose dependant (Fig. 2C and E). Consistent with previous studies on patients' muscle biopsies (22,31), *fukutin* or *fkrp* MO-injected zebrafish embryos show a reduction in glycosylated α-dystroglycan by western blot analysis (Fig. 3A) and reduced immunostaining at the vertical myoseptum (Fig. 3C and D) and notochord surrounding tissues (Fig. 4B and C) as indicated by the IIH6 antibody, which recognizes an unknown glyco-epitope that overlaps with the laminin-binding site on α-dystroglycan (40).

The motility of *fukutin* or *fkrp* MO-injected embryos is severely impaired by 48 hpf. In either case, we observed a general reduction in muscle mass associated with myotomal lesions. Unlike *sap/dmd*, *caf/lama2* or *dag1* −/− embryos, however, we found no evidence for muscle fibre detachment by labelling F-actin in *fukutin* or *fkrp* MO-injected embryos (Supplementary Material, Fig. S1). To further elucidate the muscle pathology, we assessed the sarcolemma integrity of *fukutin* and *fkrp* MO-injected embryos using EBD at 48 hpf. In contrast to *sap/dmd* −/− embryos (37), we found no evidence for muscle fibres infiltrated by EBD (Fig. 2F and G). Similar to *caf/lama2* −/− embryos (38), we detected EBD accumulation at the myotomal lesions, inter-fibre space and epithelium–muscle interface (Fig. 2F and G), indicating that sarcolemma integrity is not compromised. Together, these results suggest a distinct pathological mechanism for *fukutin* and *fkrp* MO-injected embryos that is not due to muscle fibre detachment, nor disruption of sarcolemma integrity.

Knockdown of zebrafish Fukutin or FKRP leads to notochord defects prior to muscle degeneration

Interestingly, prior to the onset of muscle degeneration, embryos injected with high doses of *fukutin* (7 ng) or *fkrp* (6 ng) MOs elicit complex phenotypes by 28 hpf, such as shortened body axes, U-shape somites and twisted notochords (Fig. 2C and E). Such myotome and notochord defects are reminiscent of those seen in zebrafish *laminin* and coatomer

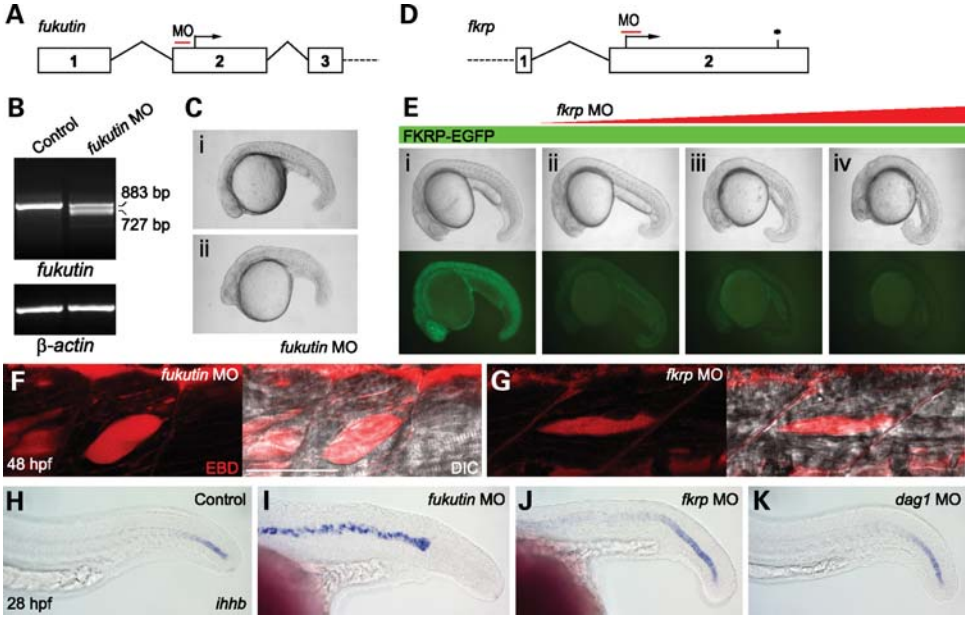

Figure 2. *fukutin* and *fkrp* MO-injected embryos are associated with notochord differentiation defects before muscle degeneration. (**A**) Schematic representation of *fukutin* MO targeting the 5′-UTR of the *fukutin* gene at the vicinity of the intron 1–exon 2 splice junction. (**B**) RT–PCR at 28 hpf and sequencing of aberrantly spliced transcripts revealed skipping of the entire exon 2 and thus the loss of translation start site. (**C**) Phenotypic severity of *fukutin* MO-injected embryos is dose dependant: (i) 4.5 ng and (ii) 7 ng at 28 hpf. (**D**) Schematic representation of *fkrp* MO targeting the translation start site of the *fkrp* gene. (**E**) Lateral view of embryos at 24 hpf after injection of 200 pg *fkrp–EGFP* mRNA (i) or together with 2 ng (ii), 4 ng (iii) or 6 ng (iv) *fkrp* MO. The phenotypic severity of *fkrp* MO-injected embryos is correlated with the concentration of *fkrp* MO, which inhibits FKRP–EGFP expression as shown under UV illumination (i–iv). (**F** and **G**) High dose *fukutin* (7 ng) and *fkrp* (6 ng) MO-injected embryos at 48 hpf. Muscle fibres visualized by DIC imaging are not infiltrated by EBD (red), which accumulates at the myotomal lesions, inter-fibre space and epithelium–muscle interface. Bar, 50 μm. (**H**–**K**) *In situ* hybridization of *ihhb* expression in the notochord at 28 hpf. In contrast to control (H) or *dag1* MO-injected embryos (K), persistent *ihhb* expression indicates that notochord cells of high-dose *fukutin* (I, 7 ng) and *fkrp* (J, 6 ng) MO-injected embryos are not fully differentiated.

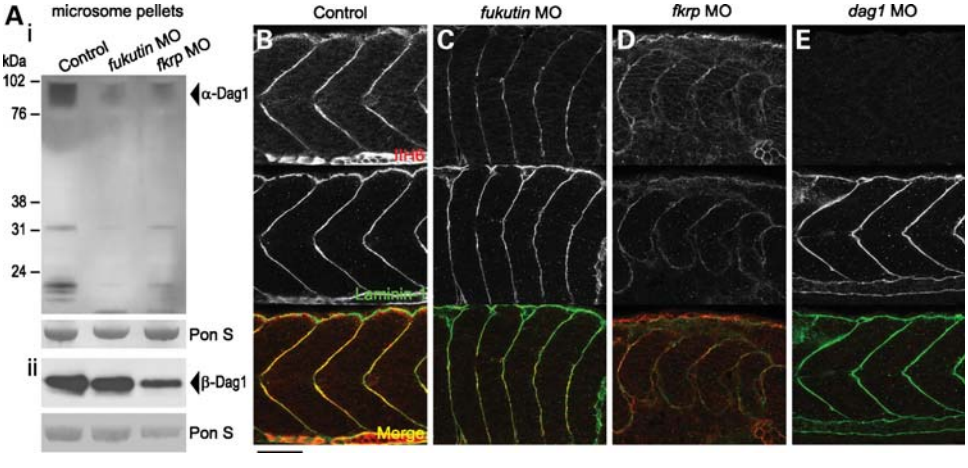

Figure 3. Glycosylated α-dystroglycan and laminin-1 immunoreactivities in the zebrafish embryos. (**A**) Western blot analysis of microsome pellets detected by the IIH6 antibody at 48 hpf (i) and β-Dag1 antibody at 28 hpf (ii). Glycosylation of α-Dag1 is reduced in *fukutin* and *fkrp* MO-injected embryos. Equal loading is shown by Ponceau S staining. (**B**–**E**) Glycosylated α-Dag1 detected by IIH6 antibody and laminin-1 immunoreactivity in control (B), *fukutin* (C), *fkrp* (D) and *dag1* (E) MO-injected embryos at 28 hpf. Glycosylated α-Dag1 is reduced in *fukutin* (C) and *fkrp* (D) MO-injected embryos and not detected in *dag1* MO-injected embryos (E). Laminin-1 immunoreactivity is strongly reduced in the posterior myoseptum of *fkrp* MO-injected embryos (D), but not affected in *fukutin* (C) or *dag1* (E) MO-injected embryos. Bar, 50 μm.

mutant embryos, two classes of mutants in which notochord cells fail to differentiate (39,41).

To test whether the abnormal notochord morphology in *fukutin* or *fkrp* MO-injected embryos is associated with a failure of notochord cell differentiation, we examined *dag1*, *fukutin* and *fkrp* MO-injected embryos using a molecular marker, *indian hedgehog homologue b* (*ihhb*), the expression of which is extinguished in fully differentiated notochords (39,41). We found that *dag1* MO-injected embryos show a slightly broader *ihhb* expression than control embryos at the tail, yet the rest of the notochord is fully differentiated (Fig. 2H and K). In contrast, the expression of *ihhb* persists

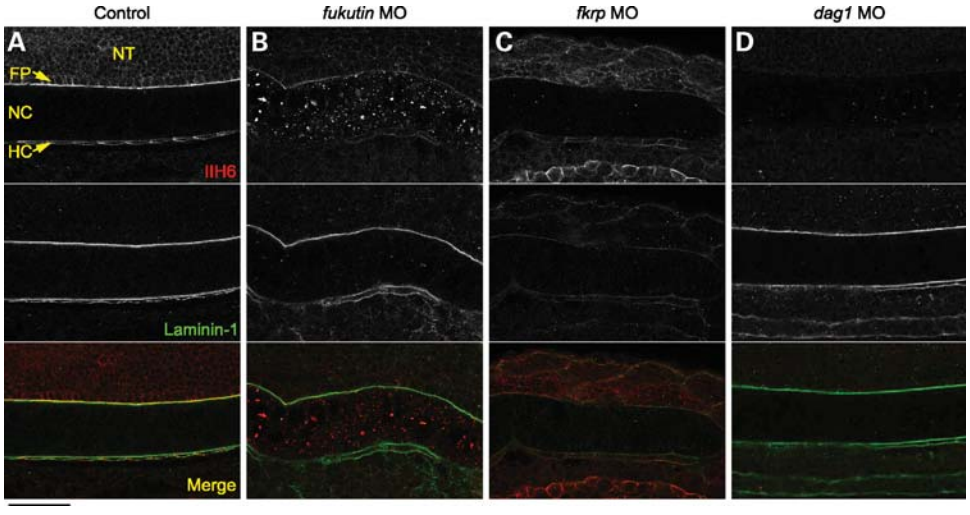

Figure 4. Glycosylated α-dystroglycan and laminin-1 immunoreactivities in the posterior notochord surrounding tissues. (**A**–**D**) Glycosylated α-dystroglycan detected by IIH6 antibody and laminin-1 immunoreactivity in control (A), *fukutin* (B), *fkrp* (C) and *dag1* (D) MO-injected embryos at 28 hpf. Glycosylated α-dystroglycan is almost absent in the NT, FP and HC in *fukutin* (B) and *fkrp* (C) MO-injected embryos and not detected in *dag1* (D) MO-injected embryos. Note that accumulation of the IIH6 epitopes was detected within the notochord cells of *fukutin* MO-injected embryos (B). Laminin-1 immunoreactivity is almost absent in the posterior FP and HC of *fkrp* MO-injected embryos (C), but not affected in *fukutin* (B) and *dag1* (D) MO-injected embryos. NT, neural tube; FP, floor plate; NC, notochord; HC, hypochord. Bar, 50 μm.

within the entire notochord in *fukutin* MO-injected embryos at 28 hpf, indicating that notochord cells fail to differentiate (Fig. 2I). Similarly, *ihhb* expression also persists in *fkrp* MO-injected embryos, although the expression level is stronger at the posterior than the anterior notochord (Fig. 2J). In addition, mid-anterior myotomes of *fkrp* MO-injected embryos tend to recover at 48 hpf, suggesting that the differentiation of anterior notochord cells may be delayed or not fully differentiated.

Laminin immunoreactivity is severely reduced in the posterior myoseptum of *fkrp* MO-injected embryos

Laminins play an essential role in notochord development. Loss of laminin-1 heterotrimer (α1β1γ1) prevents differentiation of notochord cells in zebrafish mutants, *sleepy (sly) /lamc1* and *grumpy (gup)/lamb1* (39). Following the notochord differentiation defects, we then asked whether laminin-1 immunoreactivity is affected in *fukutin* and *fkrp* MO-injected embryos. In control embryos, laminin-1 immunoreactivity is enriched at the vertical myoseptum and peri-notochord basement membrane (PBM) by 28 hpf (Figs 3B and 4A). Although *fukutin* MO-injected embryos possess shortened body axes and abnormal somite morphology, we find that laminin-1 immunoreactivity is not affected (Figs 3C and 4B). In contrast, we show that removal of FKRP causes a strong reduction in laminin-1 immunoreactivity in the posterior myoseptum (Fig. 3D) and PBM (Fig. 4C), correlated with the persistent *ihhb* expression (Fig. 2J). Consistent with *dag1* −/− embryos, laminin-1 immunoreactivity appears to be unaffected in *dag1* MO-injected embryos at 28 hpf (Figs 3E and 4D). Taken together, these results suggest that (i) FKRP may affect laminin-1 function, at least in the posterior myoseptum and (ii) knockdown of Fukutin affects notochord cell differentiation via a mechanism independent of laminin-1 function.

Knockdown of Fukutin or FKRP perturbs the expression of laminin mRNA

To investigate the loss of laminin-1 (α1β1γ1) immunoreactivity in the posterior myoseptum of *fkrp* MO-injected embryos, we examined whether knockdown of FKRP may affect expression of laminin α1, β1 and γ1 isoforms, encoded by *lama1*, *lamb1* and *lamc1*, respectively. To test this, we quantified gene expression levels of *lama1*, *lamb1* and *lamc1* in *fkrp* MO-injected embryos, compared with control embryos in addition to *fukutin* and *dag1* MO-injected embryos, as well as *sly/lamc1* −/− embryos at 28 hpf.

Compared with control embryos, we find that gene expression levels of *lama1*, *lamb1* and *lamc1* in *dag1* MO-injected embryos are not significantly up-regulated (Fig. 5A–C). In contrast, *lamc1* expression is significantly down-regulated (∼2.7-fold) in *sly/lamc1* −/− embryos, suggesting non-sense-mediated mRNA decay (Fig. 5C). In addition, expression of *lama1* and *lamb1* is significantly down-regulated in *sly/lamc1* −/− embryos (Fig. 5A and B). Surprisingly, despite a strong reduction in laminin-1 immunoreactivity in the posterior myoseptum, we find a significant up-regulation of *lama1* (∼3.8-fold), *lamb1* (∼3.2-fold) and *lamc1* (∼3.6-fold) in *fkrp* MO-injected embryos, compared with control embryos (Fig. 5A–C). Similarly, *fukutin* MO-injected embryos show a significant up-regulation of *lama1* (∼2.3-fold), *lamb1* (∼2.1-fold) and *lamc1* (∼1.5-fold) in relation to control embryos (Fig. 5A–C).

Statistical analyses indicate that up-regulated *lama1*, *lamb1* and *lamc1* expression in *fukutin* and *fkrp* MO-injected embryos is significantly different from that in *dag1* MO-injected embryos (Fig. 5A–C) and down-regulated

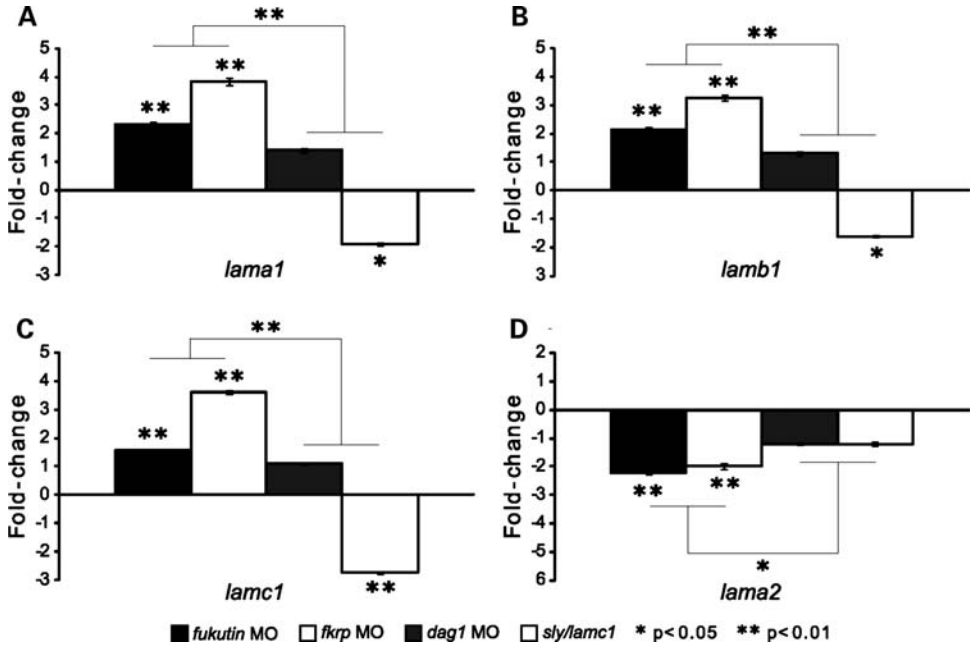

Figure 5. Quantification of laminin isoform gene expression levels. Expression levels of *lama1* (**A**), *lamb1* (**B**), *lamc1* (**C**) and *lama2* (**D**), normalized to *β-actin* expression in *fukutin*, *fkrp* and *dag1* MO-injected, as well as *sly/lamc1* −/− embryos at 28 hpf. Each coloured bar represents the mean of fold-changes in relation to control (buffer-injected) embryos, set as 1. Error bars represent standard error of the mean (SEM). Statistical significance is indicated by asterisks.

lama1, *lamb1* and *lamc1* expression in *sly/lamc1* −/− embryos (Fig. 5A–C). Together, these results suggest that removal of Fukutin or FKRP, but not dystroglycan perturbs the gene expression levels of laminin isoforms.

Expression of *laminin α2* is selectively down-regulated in *fukutin* or *fkrp* MO-injected embryos

Dystroglycanopathies due to mutations in *fukutin* or *fkrp* may be associated with a reduction in laminin α2 isoform (a ligand of dystroglycan), as shown by western blot or immunostaining (31,42). To test whether the reduction in laminin α2 may be due to perturbation of transcription or disruption of dystroglycan–ligand interactions, we quantified the gene expression level of *lama2* in *fukutin* and *fkrp* MO-injected embryos, compared with control and *dag1* MO-injected embryos at 28 hpf. Without laminin γ1, laminin α2 cannot form functional heterotrimer laminin-2 (α2β1γ1) in *sly/lamc1* −/− embryos (39). Thus, apart from *dag1* MO-injected embryos, *sly/lamc1* −/− embryos are used for representing disruption of dystroglycan–ligand interactions.

Here we show that, compared with control embryos, *lama2* gene expression is not significantly down-regulated in either *dag1* MO-injected or *sly/lamc1* −/− embryos (Fig. 5D). Interestingly, removal of Fukutin or FKRP causes a significant down-regulation of *lama2* expression (∼2-fold) in relation to control embryos (Fig. 5D). In addition, down-regulated *lama2* expression in *fukutin* and *fkrp* MO-injected embryos is significantly different from that in *dag1* MO-injected or *sly/lamc1* −/− embryos (Fig. 5D). In sum, our results are consistent with the previously reported reduction in laminin α2 isoform in Fukutin- or FKRP-deficient dystroglycanopathy patients (31,42), yet down-regulation of *lama2* gene expression is not due to disruption of dystroglycan–ligand interactions, suggesting an alternative pathological mechanism.

Knockdown of Fukutin or FKRP may affect protein secretion beyond glycosylation of α-dystroglycan

The coatomer vesicular complex is essential for maintenance of the Golgi and secretory activities in eukaryotic cells. Loss of coatomer function leads to notochord differentiation defects in zebrafish coat protein complex I mutants (41). As Fukutin and FKRP are putative glycosyltransferases in the secretory pathway, we wondered whether notochord defects in *fukutin* and *fkrp* MO-injected embryos might be due to abnormal secretion. In contrast to a severe reduction in glycosylated α-dystroglycan in the neural tube, floor plate and hypochord, we frequently detected accumulation of IIH6 epitopes in the notochord cells of *fukutin* and *fkrp* MO-injected embryos (Figs 4B and 6E and F). We speculated that the accumulated IIH6 epitopes might be unsecreted dystroglycan and asked whether removing the dystroglycan propeptide would eliminate accumulation of IIH6 epitopes in *fukutin* or *fkrp* MO-injected embryos. We show that *fukutin* and *dag1* MO-co-injected embryos resemble loss-of-Fukutin morphology (Fig. 6B and C). The accumulation of IIH6 epitopes caused by knockdown of Fukutin is still detected, even in the absence of dystroglycan (indicated by the absence of immunoreactivity in the notochord surrounding tissues) (Fig. 6B and C). Similar results were also observed in *fkrp* and *dag1* MO-co-injected embryos (data not shown). Together, these results suggest that *fukutin* and *fkrp* are epistatic to *dag1* and implicate that accumulated IIH6 epitopes may be present on other proteins in the notochord cells.

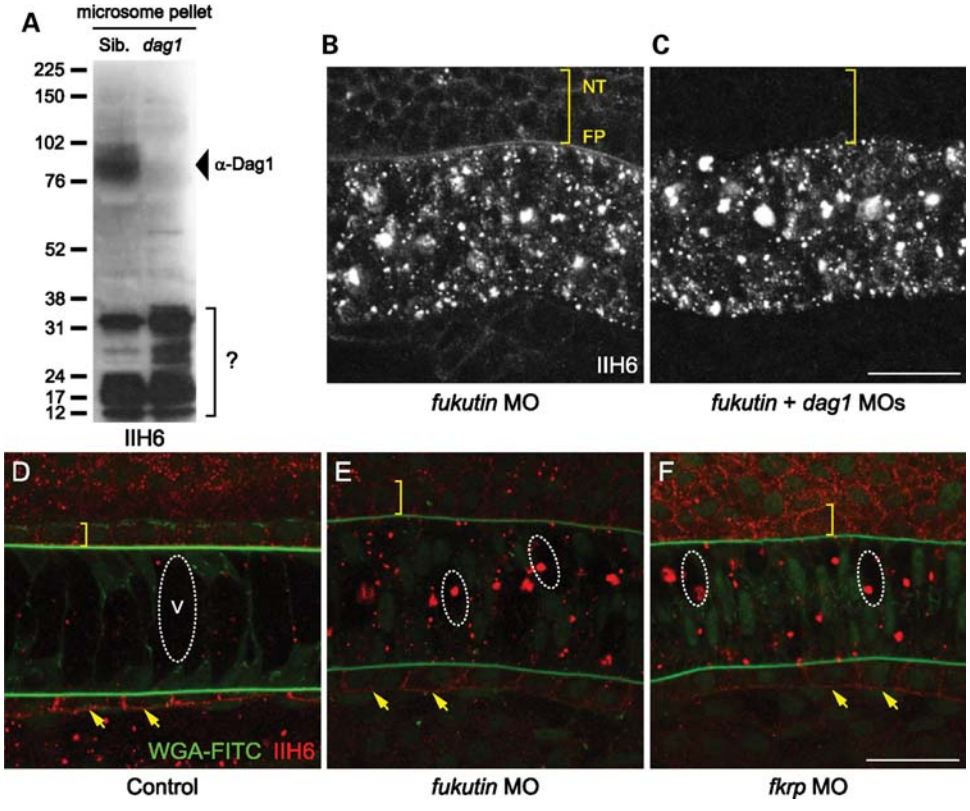

Figure 6. Knockdown of Fukutin or FKRP may affect protein secretion beyond glycosylation of α-dystroglycan. (**A**) Western blot analysis of microsome pellets detected by the IIH6 antibody. Glycosylated α-Dag1 is absent in *dag1* −/− embryos. Nevertheless, low molecular-weight unknown proteins were detected by the IIH6 antibody. (**B** and **C**) *fukutin* and *dag1* MO-co-injected embryos resemble loss-of-Fukutin morphology. Although dystroglycan is not detected in the notochord surrounding tissues (bracket, C), accumulation of IIH6 epitopes is still detected in the notochord cells. (**D**–**F**) IIH6 epitopes in the notochord cells are not labelled by WGA-FITC and mainly accumulate in the vacuoles (dashed circles) in *fukutin* and *fkrp* MO-injected embryos. Cell size is enlarged in the floor plate (brackets) and hypochord (arrows). NT, neural tube; FP, floor plate; V, vacuole. Bar, 25 μm.

Additional assessments further confirm that the IIH6 epitope is not only present on α-dystroglycan, which also carries the *N*-acetylglucosamine modification that can be recognized by wheat germ agglutinin (WGA). In *dag1* −/− embryos, western blot analysis using the IIH6 antibody reveals several low molecular-weight bands in microsome pellets, but not in glycoproteins enriched by WGA beads (Figs 1E and 6A). In addition, we ask whether fluorescein isothiocyanate (FITC)-conjugated WGA may co-localize with accumulated IIH6 epitopes in the notochord cells. We show that WGA-FITC labels the PBM and Golgi apparatus in control embryos (Fig. 6D), whereas IIH6 epitopes in the notochord cells are not labelled by WGA-FITC and mainly accumulate in the vacuoles in *fukutin* and *fkrp* MO-injected embryos (Fig. 6E and F). Based on these results, we infer that knockdown of Fukutin or FKRP may, directly or indirectly, affect protein secretion beyond glycosylation of α-dystroglycan.

Knockdown of Fukutin or FKRP causes ER stress and activates the UPR

The first compartment of the secretory pathway is the ER, where transmembrane and secreted proteins fold into their native confirmation and post-translationally modified. Influx of nascent, unfolded polypeptides causes ER stress. Signal transduction pathways maintaining the homeostasis of the ER are termed as the UPR, which involve changes in gene transcription in stressed cells (reviewed in 43,44). Here we examined the possibility that removal of Fukutin family proteins may cause ER stress and activate the UPR. A classical marker for UPR activation is BiP/GRP78, the most abundant chaperone that regulates all three UPR signalling branches by binding to unfolded proteins in the ER lumen (43,44). We quantified the gene expression level of *bip* in *fukutin* and *fkrp* MO-injected embryos, compared with control embryos in addition to *dag1* MO-injected and *sly/lamc1* −/− embryos, which represent disruption of dystroglycan–ligand interactions.

Here we show that *bip* expression in *dag1* MO-injected and *sly/lamc1* −/− embryos are not significantly different from control embryos. In contrast, *bip* expression is significantly up-regulated by ∼3-fold in *fukutin* or *fkrp* MO-injected embryos at 28 hpf, compared with control embryos as well as *dag1* MO-injected and *sly/lamc1* −/− embryos (Fig. 7A). One branch of the UPR is regulated through transcription factor XBP1 activation, which requires an unconventional splicing (44). We show that increased *XBP1* unconventional splicing was detected in *fukutin* or *fkrp* MO-injected embryos (Supplementary Material, Fig. S5). GYLTL1B, a putative glycosyltransferase also known as

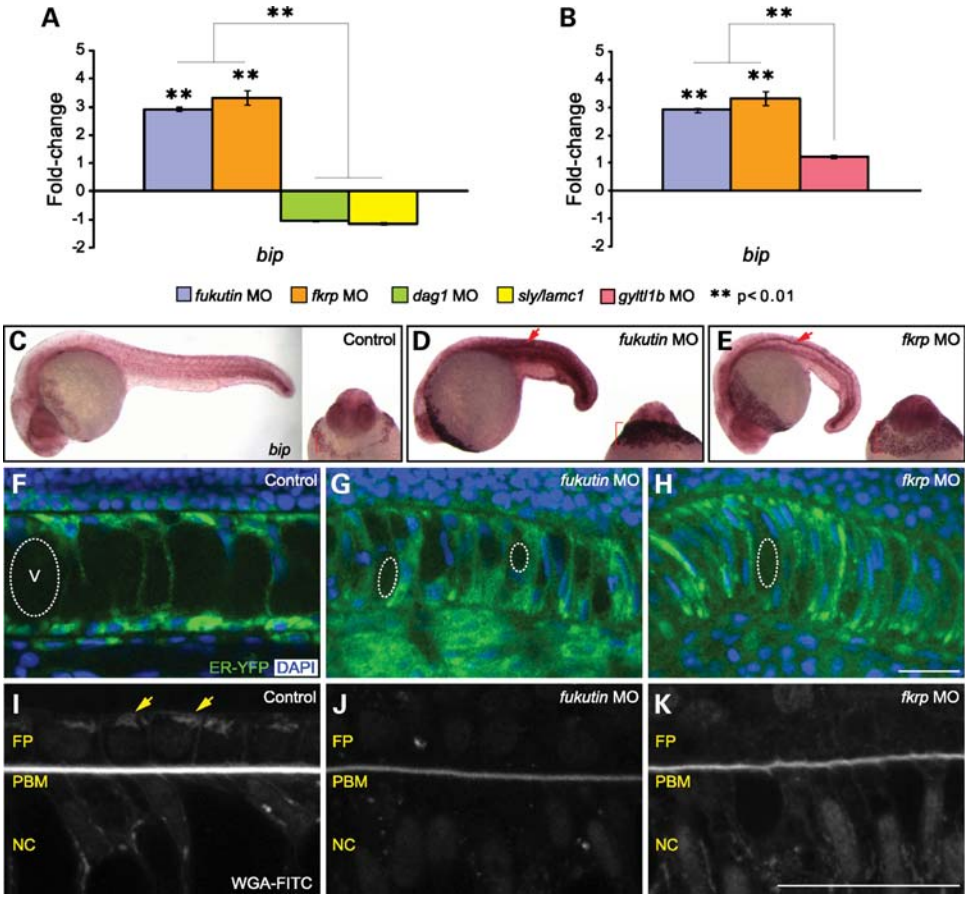

Figure 7. UPR activation and ER stress in zebrafish embryos lacking Fukutin or FKRP. (**A** and **B**) Quantification of *bip* expression (normalized to *β-actin* expression) in *fukutin*, *fkrp*, *dag1* and *gyltl1b* MO-injected and *sly/lamc1* −/− embryos at 28 hpf. Each coloured bar represents the mean of fold-changes in relation to control embryos. Error bars: SEM. (**C**–**E**) *bip in situ* hybridization at 28 hpf. Widespread up-regulation of *bip* is detected in *fukutin* (D) and *fkrp* (E) MO-injected embryos, particularly in the floor plate (arrows) and expanded hatching gland (brackets). (**F**–**H**) Remarkable ER expansion in *fukutin* (G) or *fkrp* (H) MO-injected embryos associated with abnormal nuclei and reduced notochord vacuole size (dashed circles). (**I**–**K**) No discernable structure of WGA-FITC-labelled Golgi apparatus (arrows, I) was identified in the neural floor plate or notochord cells of *fukutin* (J) or *fkrp* (K) MO-injected embryos, which are associated with decreased levels of WGA-FITC-labelled PBM. V, vacuole; FP, floor plate; PBM, peri-notochord basement membrane; NC, notochord. Bar, 25 μm.

LARGE2, was identified to stimulate *O*-glycosylation of α-dystroglycan in cultured cells (45,46). Similar to *dag1* MO-injected embryos, the IIH6 immunostaining is almost absent in *gyltl1b* MO-injected embryos, whereas laminin-1 localization is not affected (Supplementary Material, Fig. S2). Absence of the IIH6 epitope implicates loss of the ligand interaction site on dystroglycan. As an additional comparison, we find that *bip* expression in *gyltl1b* MO-injected embryos is similar to control embryos and significantly lower than up-regulated *bip* in *fukutin* or *fkrp* MO-injected embryos (Fig. 7B).

Analysis of *bip* gene expression suggests that knockdown of Fukutin or FKRP, but not disruption of dystroglycan–ligand interactions is responsible for activation of the UPR. Next, we examine whether the UPR in *fukutin* or *fkrp* MO-injected embryos may be restricted in specific tissues. By *in situ* hybridization, we find a ubiquitous up-regulation of *bip* expression in *fukutin* and *fkrp* MO-injected embryos. Nevertheless, the most intense signal is detected in the neural floor plate and expanded hatching gland at 28 hpf (Fig. 7C–E), both then diminished by 48 hpf (Supplementary Material, Fig. S3).

The size of the ER correlates with the unfolded protein load across cell types and the UPR contributes to the coupling of ER expansion to ER stress (44). To assess ER stress in *fukutin* or *fkrp* MO-injected embryos, an ER–yellow fluorescent protein (YFP) marker was co-injected to indicate the size of the ER. Compared with unstressed ER around the nuclei in control embryos (Fig. 7F), we find remarkable expansion of the ER in *fukutin* or *fkrp* MO-injected embryos, especially in the notochord cells where vacuoles fail to inflate properly and nuclei possess abnormal shape (Fig. 7G and H). In addition, enlarged cell size in the floor plate and hypochord is correlated with the expanded ER (Fig. 6E and F). We show that levels of WGA-FITC-labelled PBM are strongly decreased in *fukutin* or *fkrp* MO-injected embryos in which no discernable structure of WGA-FITC-labelled Golgi apparatus was identified in the neural floor plate or notochord cells, suggesting fragmented or altered Golgi morphology in response to ER stress (Fig. 7I–K). Taken

together, these results suggest that knockdown of Fukutin or FKRP causes ER stress and activation of the UPR before disruption of dystroglycan–ligand interactions.

DISCUSSION

In this study, we have modelled dystroglycanopathies in zebrafish by characterization of a novel *dag1* loss-of-function allele and inhibition of Fukutin family protein activities. Mutations in *dystroglycan*, which may lead to embryonic lethality, have not been identified yet to cause human muscular dystrophy, whereas mutations in *fukutin* or *fkrp* are most commonly responsible for dystroglycanopathies in humans. Two groups previously showed that *fkrp* MO-injected zebrafish embryos recapitulate α-dystroglycan glycosylation defect and thus are suitable for modelling human dystroglycanopathies (47,48). By comparing *dag1* mutant allele with *fukutin* and *fkrp* MO-injected embryos, for the first time, we are able to distinguish differences in their muscle pathology and dissect the underlying molecular and cellular mechanisms.

First, we have shown that a complete absence of dystroglycan leads to dislocated dystrophin associated with free ends of detached muscle fibres, whereas laminin localization remains unaffected in zygotic *dag1* −/− zebrafish. Interestingly, dystrophin immunoreactivity cannot be detected in *dag1* MO-injected embryos, in which translation of maternal *dag1* transcript is inhibited, while laminin immunoreactivity is unaffected (49). We reason that lack of maternally supplied dystroglycan may lead to a loss of dystrophin, but laminin localization is unchanged. In contrast to previous findings that hypoglycosylated α-dystroglycan in patients and *fkrp* MO-injected embryos leads to reduced dystroglycan–laminin-binding activity *in vitro* (22,47,48), our results are consistent with the dystroglycan-deficient chimaeric mice which develop muscular dystrophy with decreased levels of dystrophin, whereas basement membranes and the deposition of laminins remain unaffected (50). In addition, analyses have shown that dystrophin immunoreactivity is essentially normal in muscle biopsies of most FCMD patients (42,51,52), as it is in *fukutin* and *fkrp* MO-injected embryos (data not shown), suggesting that pathological mechanisms different from a complete absence of dystroglycan or disruption of dystroglycan–ligand interactions could be involved (see below).

Second, we have shown that removing Fukutin or FKRP in zebrafish causes notochord differentiation defects and perturbs expression of laminins before muscle degeneration. Notably, aberrant expression of laminin α5 was reported to be detected around most muscle fibres in FCMD patients, whereas it was rarely detected in control muscle biopsies (42,53). Together, these results raise the possibility that changes of laminin isoform expression may lead to abnormal laminin polymerization and assembly within the basement membrane. Indeed, fragility in basal lamina has been reported in the brain of FCMD and *fkrp* mutation-associated WWS and MEB patients (54–57). In addition, Fukutin-deficient chimaeric mice show disorganized laminar structure in the brain and retina (58); similar results have been shown in homozygote Fkrp-Neo (Tyr307Asn) mice, which have reduced levels of *fkrp* transcript (59).

Third, we have shown that knockdown of Fukutin family proteins, but not disruption of dystroglycan–ligand interactions causes ER stress and activation of UPR. UPR is an evolutionarily conserved mechanism allowing the ER to recover from the accumulation of unfolded proteins mainly by (i) down-regulation of genes encoding secreted proteins and increasing the transcription of genes that contribute to ER function, (ii) reducing translation initiation and (iii) increasing the clearance of misfolded proteins through ER-associated degradation (ERAD) (43,60,61). Intriguingly, disruption of Fukutin or FKRP expression leads to accumulated IIH6 epitopes (Fig. 6), which are not present on α-dystroglycan and probably sequestered into the notochord vacuoles by a mechanism similar to autophagy in UPR-activated cells to ease ER stress (62,63). Here we propose a model for dystroglycanopathies linked with the UPR (Fig. 8). In the normal condition, when dystroglycan is misfolded, the UPR acts as the quality control machinery to ensure proper folding and secretion of glycosylated dystroglycan. Our result indicate, however, that in dystroglycanopathies, knockdown of Fukutin or FKRP function may affect protein secretion beyond glycosylation of α-dystroglycan, resulting in acute ER stress and the activation of UPR. Subsequent signalling events as part of the UPR to ease the ER stress include changes in gene transcription, ERAD and translational repression. When the stress remains overwhelming, cell death pathways may be activated. Hypoglycosylated dystroglycan may be secreted to the plasma membrane, yet its interactions with ligands in the extracellular matrix are disrupted.

It is becoming evident that the extent of hypoglycosylated α-dystroglycan as judged by IIH6 immunostaining may not be the only factor contributing to the clinical severity of patients carrying *fukutin* or *FKRP* mutations (64). In addition, *fukutin* and *fkrp* mutations can perturb sarcolemma-associated proteins beyond α-dystroglycan (51,65). We reason that variable immunoreactivities of DGC components in *fukutin* or *fkrp* mutation-associated dystroglycanopathies may reflect distinct consequences from ER stress and activation of UPR. Significantly, the UPR may be responsible for the pathological mechanism that contributes to the wide spectrum of clinical severity in dystroglycanopathies. In fact, a wide variety of diseases have been associated with malfunction of the ER and defective UPR signalling, including Marinesco–Sjögren syndrome, a cerebellar ataxia with cataract and myopathy, caused by mutations in *SIL1* that encodes a nucleotide exchange factor for BiP (66). In addition, intense UPR signal in the neural floor plate of *fukutin* and *fkrp* MO-injected embryos is also consistent with the central nervous system involvement in some dystroglycanopathy patients (4,10).

Up-regulation of BiP/GRP78 was reported in muscle biopsies from LGMD2I patients (67). To verify this result, we have studied muscle biopsies from patients with a number of molecularly characterized dystroglycanopathies. We indeed detected activation of the UPR in some dystroglycanopathy patients with mutations in *fukutin* or *fkrp*. The activation of the UPR was, however, not a universal finding (our unpublished results). We reasoned that the difference between the zebrafish and the human results could be related to different factors: (i) the clinical severity and genetic background of the population studied was heterogeneous, unlike the

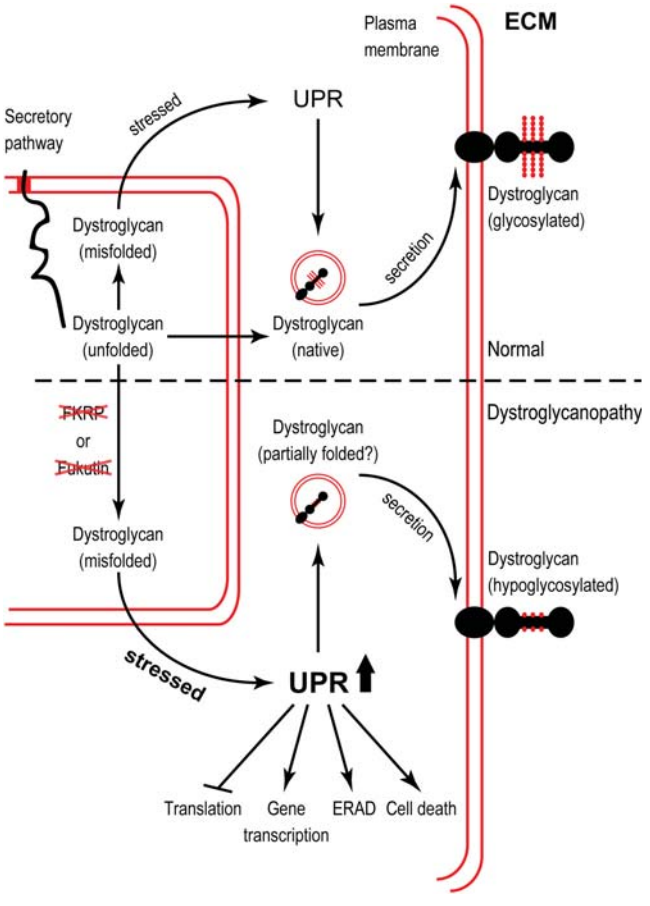

Figure 8. A model for dystroglycanopathies linked with the UPR. Normal condition and dystroglycanopathies are separated by the dashed line. Double red lines represent the lipid bilayer. Relevant stages of post-translational processing of dystroglycan are indicated. Knockdown of Fukutin or FKRP causes ER stress and activation of the UPR, preceding loss of dystroglycan–ligand interactions. UPR, unfolded protein response; ECM, extracellular matrix; ERAD, ER-associated degradation.

zebrafish; in particular, hypomorphic alleles may retain residual function, allowing patients to ease the ER stress; thus, the UPR marker detected at a late time point is lower than expected, (ii) the timing at which a muscle biopsy was obtained. During the progression of muscular dystrophy, muscle cells in different patients are replaced by connective tissue and fat to different degrees; thus, the detection of UPR needs to be normalized according to the residual muscle mass on muscle biopsies, and (iii) muscle biopsies may not be the ideal tissue to detect subtle UPR activation. In fact, the strongest signal of the UPR activation in the zebrafish models of dystroglycanopathies is detected in the neural floor plate prior to muscle differentiation. This suggests that a different approach and availability of different tissues is required to further investigate the UPR in dystroglycanopathy patients.

In sum, the zebrafish provide valuable models for studying the pathophysiological aspects of dystroglycanopathies. While it remains unclear whether Fukutin and FKRP are bona fide glycosyltransferases, our study suggests important roles for Fukutin family proteins in the secretory pathway and that the UPR may contribute to the wide phenotypic spectrum of some dystroglycanopathies in humans. Further studies of the roles of Fukutin and FKRP in the secretory pathway will provide new insights into the molecular mechanisms that are critical for the organs targeted in some dystroglycanopathies and help development of therapeutic strategies that ease ER stress.

MATERIALS AND METHODS

Antisense MOs and constructs

Unless otherwise stated, MOs (Gene Tools) were injected into 1- or 2-cell-stage embryos with dosages specified below. Standard control MO (7 ng), *dag1* MO (7 ng) and *gyltl1b/large2* MO (6 ng) have been described (49,68). MOs used in this study: *fukutin* MO (5′-AGCAGCCTCATATCTGTGCCC AGAA-3′, 7 ng); *fkrp* MO (5′-CTGGCAAAAACTGATA CGCATTATG-3′, 6 ng). Zebrafish *fkrp* coding sequence was cloned in front of the *egfp* coding sequence to generate in-frame *fkrp–egfp* construct and make mRNA for injection. ER–YFP vector (Clontech) encodes a fluorescent fusion protein carrying Calreticulin ER targeting and lysine-aspartate-glutamate-leucine retrieval sequences. ER–YFP mRNA was made and injected (200 pg) alone or with MOs.

EBD, Acridine Orange and *in situ* hybridization

As previously described (37,38), 0.1% EBD (Sigma) and 5 μg/ml Acridine Orange (AO, Sigma) were injected into the peri-cardic sinus of zebrafish embryos by 48 hpf, allowing EBD or AO circulated through the cardiovascular system before analysis under confocal microscopy. *In situ* hybridization for *ihhb* expression was carried out as described (69,70).

Immunohistochemistry

Protocols for the following primary antibodies have been described (49): rabbit anti-laminin (Sigma L-9393; 1:400), mouse anti-β-Dag1 (Novocastra 43DAG1/8D5; 1:50) and anti-dystrophin (Sigma MANDRA-1; 1:100). For anti-α-Dag1 (IIH6 epitope, gift from K. Campbell; 1:50), embryos were fixed in 4% paraformaldehyde (PFA) overnight at 4°C, followed by 100% methanol. Fluorescent secondary antibodies (Molecular Probes; 1:250) used in this study are Alexa 488 anti-mouse or anti-rabbit immunoglobulin G (IgG); Alexa 594 anti-mouse IgG or immunoglobulin M. WGA-FITC (Sigma; 10 μg/ml) was used for detecting *N*-glycans and Golgi apparatus. For labelling F-actin, embryos were fixed for 2 h at room temperature in 4% PFA, followed by four washes of 2% Triton X-100/phosphate-buffered saline and incubation in Alexa 488 phalloidin (Molecular Probes; 1:100) overnight at 4°C.

Microsome preparation, glycoprotein enrichment and western blot analysis

Zebrafish embryos were homogenized in pyrophosphate buffer containing protease inhibitors cocktail (Roche) and centrifuged at 14 000*g*. The supernatant was then ultra-centrifuged

at 142 000*g* to obtain microsome pellet, which was then solubilised in wash buffer (Tris-buffered saline containing 0.1% Triton X-100 and protease inhibitors). The solubilised fraction can either proceed to western blot analysis or incubate with WGA beads (Vector Labs) overnight at 4°C for glycoprotein enrichment. WGA beads were washed three times in wash buffer, followed by elution with 0.3 M *N*-acetylglucosamine in wash buffer. Proteins were separated by 4–12% Bis–Tris gels (Invitrogen); transferred to polyvinylidene fluoride membranes (Immobilon); probed with IIH6 antibody (1:2000), anti-acetylated tubulin (1:1000) or anti-β-Dag1 (1:50) and developed with horseradish peroxidise-enhanced chemiluminescence (Pierce).

Quantitative real-time PCR and statistical analysis

Total RNA was extracted from control and MO-injected embryos using TRIzol (Invitrogen). First-strand cDNA was synthesized using random primers and SuperScript II (Invitrogen). Taqman probes (Applied Biosystems) were used for quantifying gene expression levels of *lama1*, *lamb1*, *lamc1*, *lama2*, *bip* and *β-actin* (Supplementary Material, Table S1). Quantitative PCR was carried out for three biological repeats with measurements taken from three technical repeats, followed by one-way analysis of variance and Tukey honestly significantly different test.

SUPPLEMENTARY MATERIAL

Supplementary Material is available at *HMG* online.

ACKNOWLEDGEMENTS

We thank Kevin Campbell, Aaron Beedle and Susan Brown for critical comments on the manuscript and Jeffrey Barrett for help with statistical analysis. For providing the zebrafish knockout allele, *dag1*^{hu3072}, we thank the Hubrecht laboratory and the Sanger Institute Zebrafish Mutation Resource.

Conflict of Interest statement. None declared.

FUNDING

This work was supported by ZF-MODELS Integrated Project; contract number LSHG-CT-2003-503496; funded by the European Commission. This work was also sponsored by the Wellcome Trust (grant number WT 077047/Z/05/Z) and (grant number WT 077037/Z/05/Z). We wish also to thank the MRC Neuromuscular Centre Biobank, and the MDC Centre Grant to F.M. Funding to pay the Open Access publication charges for this article was provided by Wellcome Trust Sanger Institute.

REFERENCES

1. Helbling-Leclerc, A., Zhang, X., Topaloglu, H., Cruaud, C., Tesson, F., Weissenbach, J., Tome, F.M., Schwartz, K., Fardeau, M., Tryggvason, K. *et al.* (1995) Mutations in the laminin alpha 2-chain gene (LAMA2) cause merosin-deficient congenital muscular dystrophy. *Nat. Genet.*, **11**, 216–218.
2. Pegoraro, E., Marks, H., Garcia, C.A., Crawford, T., Mancias, P., Connolly, A.M., Fanin, M., Martinello, F., Trevisan, C.P., Angelini, C. *et al.* (1998) Laminin alpha2 muscular dystrophy: genotype/phenotype studies of 22 patients. *Neurology*, **51**, 101–110.
3. Tome, F.M., Evangelista, T., Leclerc, A., Sunada, Y., Manole, E., Estournet, B., Barois, A., Campbell, K.P. and Fardeau, M. (1994) Congenital muscular dystrophy with merosin deficiency. *C. R. Acad. Sci. III*, **317**, 351–357.
4. Jimenez-Mallebrera, C., Brown, S.C., Sewry, C.A. and Muntoni, F. (2005) Congenital muscular dystrophy: molecular and cellular aspects. *Cell Mol. Life Sci.*, **62**, 809–823.
5. Allamand, V., Sunada, Y., Salih, M.A., Straub, V., Ozo, C.O., Al-Turaiki, M.H., Akbar, M., Kolo, T., Colognato, H., Zhang, X. *et al.* (1997) Mild congenital muscular dystrophy in two patients with an internally deleted laminin alpha2-chain. *Hum. Mol. Genet.*, **6**, 747–752.
6. Naom, I., D'Alessandro, M., Sewry, C.A., Jardine, P., Ferlini, A., Moss, T., Dubowitz, V. and Muntoni, F. (2000) Mutations in the laminin alpha2-chain gene in two children with early-onset muscular dystrophy. *Brain*, **123**, 31–41.
7. Naom, I., D'Alessandro, M., Sewry, C.A., Philpot, J., Manzur, A.Y., Dubowitz, V. and Muntoni, F. (1998) Laminin alpha 2-chain gene mutations in two siblings presenting with limb-girdle muscular dystrophy. *Neuromuscul. Disord.*, **8**, 495–501.
8. Tan, E., Topaloglu, H., Sewry, C., Zorlu, Y., Naom, I., Erdem, S., D'Alessandro, M., Muntoni, F. and Dubowitz, V. (1997) Late onset muscular dystrophy with cerebral white matter changes due to partial merosin deficiency. *Neuromuscul. Disord.*, **7**, 85–89.
9. Brockington, M., Yuva, Y., Prandini, P., Brown, S.C., Torelli, S., Benson, M.A., Herrmann, R., Anderson, L.V., Bashir, R., Burgunder, J.M. *et al.* (2001) Mutations in the fukutin-related protein gene (FKRP) identify limb girdle muscular dystrophy 2I as a milder allelic variant of congenital muscular dystrophy MDC1C. *Hum. Mol. Genet.*, **10**, 2851–2859.
10. Godfrey, C., Clement, E., Mein, R., Brockington, M., Smith, J., Talim, B., Straub, V., Robb, S., Quinlivan, R., Feng, L. *et al.* (2007) Refining genotype phenotype correlations in muscular dystrophies with defective glycosylation of dystroglycan. *Brain*, **130**, 2725–2735.
11. Ibraghimov-Beskrovnaya, O., Ervasti, J.M., Leveille, C.J., Slaughter, C.A., Sernett, S.W. and Campbell, K.P. (1992) Primary structure of dystrophin-associated glycoproteins linking dystrophin to the extracellular matrix. *Nature*, **355**, 696–702.
12. Holt, K.H., Crosbie, R.H., Venzke, D.P. and Campbell, K.P. (2000) Biosynthesis of dystroglycan: processing of a precursor propeptide. *FEBS Lett.*, **468**, 79–83.
13. Gee, S.H., Montanaro, F., Lindenbaum, M.H. and Carbonetto, S. (1994) Dystroglycan-alpha, a dystrophin-associated glycoprotein, is a functional agrin receptor. *Cell*, **77**, 675–686.
14. Sugiyama, J., Bowen, D.C. and Hall, Z.W. (1994) Dystroglycan binds nerve and muscle agrin. *Neuron*, **13**, 103–115.
15. Hohenester, E., Tisi, D., Talts, J.F. and Timpl, R. (1999) The crystal structure of a laminin G-like module reveals the molecular basis of alpha-dystroglycan binding to laminins, perlecan, and agrin. *Mol. Cell*, **4**, 783–792.
16. Talts, J.F., Andac, Z., Gohring, W., Brancaccio, A. and Timpl, R. (1999) Binding of the G domains of laminin alpha1 and alpha2 chains and perlecan to heparin, sulfatides, alpha-dystroglycan and several extracellular matrix proteins. *EMBO J.*, **18**, 863–870.
17. Sato, S., Omori, Y., Katoh, K., Kondo, M., Kanagawa, M., Miyata, K., Funabiki, K., Koyasu, T., Kajimura, N., Miyoshi, T. *et al.* (2008) Pikachurin, a dystroglycan ligand, is essential for photoreceptor ribbon synapse formation. *Nat. Neurosci.*, **11**, 923–931.
18. Sugita, S., Saito, F., Tang, J., Satz, J., Campbell, K. and Sudhof, T.C. (2001) A stoichiometric complex of neurexins and dystroglycan in brain. *J. Cell Biol.*, **154**, 435–445.
19. Barresi, R. and Campbell, K.P. (2006) Dystroglycan: from biosynthesis to pathogenesis of human disease. *J. Cell Sci.*, **119**, 199–207.
20. Kim, D.S., Hayashi, Y.K., Matsumoto, H., Ogawa, M., Noguchi, S., Murakami, N., Sakuta, R., Mochizuki, M., Michele, D.E., Campbell, K.P. *et al.* (2004) POMT1 mutation results in defective glycosylation and loss of laminin-binding activity in alpha-DG. *Neurology*, **62**, 1009–1011.
21. Longman, C., Brockington, M., Torelli, S., Jimenez-Mallebrera, C., Kennedy, C., Khalil, N., Feng, L., Saran, R.K., Voit, T., Merlini, L. *et al.* (2003) Mutations in the human LARGE gene cause MDC1D, a novel form of congenital muscular dystrophy with severe mental retardation and

abnormal glycosylation of alpha-dystroglycan. *Hum. Mol. Genet.*, **12**, 2853–2861.
22. Michele, D.E., Barresi, R., Kanagawa, M., Saito, F., Cohn, R.D., Satz, J.S., Dollar, J., Nishino, I., Kelley, R.I., Somer, H. *et al.* (2002) Post-translational disruption of dystroglycan-ligand interactions in congenital muscular dystrophies. *Nature*, **418**, 417–422.
23. Chiba, A., Matsumura, K., Yamada, H., Inazu, T., Shimizu, T., Kusunoki, S., Kanazawa, I., Kobata, A. and Endo, T. (1997) Structures of sialylated O-linked oligosaccharides of bovine peripheral nerve alpha-dystroglycan. The role of a novel O-mannosyl-type oligosaccharide in the binding of alpha-dystroglycan with laminin. *J. Biol. Chem.*, **272**, 2156–2162.
24. Sasaki, T., Yamada, H., Matsumura, K., Shimizu, T., Kobata, A. and Endo, T. (1998) Detection of O-mannosyl glycans in rabbit skeletal muscle alpha-dystroglycan. *Biochim. Biophys. Acta*, **1425**, 599–606.
25. Smalheiser, N.R., Haslam, S.M., Sutton-Smith, M., Morris, H.R. and Dell, A. (1998) Structural analysis of sequences O-linked to mannose reveals a novel Lewis X structure in cranin (dystroglycan) purified from sheep brain. *J. Biol. Chem.*, **273**, 23698–23703.
26. Yoshida-Moriguchi, T., Yu, L., Stalnaker, S.H., Davis, S., Kunz, S., Madson, M., Oldstone, M.B., Schachter, H., Wells, L. and Campbell, K.P. (2010) O-mannosyl phosphorylation of alpha-dystroglycan is required for laminin binding. *Science*, **327**, 88–92.
27. Beltran-Valero de Bernabe, D., Currier, S., Steinbrecher, A., Celli, J., van Beusekom, E., van der Zwaag, B., Kayserili, H., Merlini, L., Chitayat, D., Dobyns, W.B. *et al.* (2002) Mutations in the O-mannosyltransferase gene POMT1 give rise to the severe neuronal migration disorder Walker-Warburg syndrome. *Am. J. Hum. Genet.*, **71**, 1033–1043.
28. van Reeuwijk, J., Janssen, M., van den Elzen, C., Beltran-Valero de Bernabe, D., Sabatelli, P., Merlini, L., Boon, M., Scheffer, H., Brockington, M., Muntoni, F. *et al.* (2005) POMT2 mutations cause alpha-dystroglycan hypoglycosylation and Walker-Warburg syndrome. *J. Med. Genet.*, **42**, 907–912.
29. Yoshida, A., Kobayashi, K., Manya, H., Taniguchi, K., Kano, H., Mizuno, M., Inazu, T., Mitsuhashi, H., Takahashi, S., Takeuchi, M. *et al.* (2001) Muscular dystrophy and neuronal migration disorder caused by mutations in a glycosyltransferase, POMGnT1. *Dev. Cell*, **1**, 717–724.
30. Kobayashi, K., Nakahori, Y., Miyake, M., Matsumura, K., Kondo-Iida, E., Nomura, Y., Segawa, M., Yoshioka, M., Saito, K., Osawa, M. *et al.* (1998) An ancient retrotransposal insertion causes Fukuyama-type congenital muscular dystrophy. *Nature*, **394**, 388–392.
31. Brockington, M., Blake, D.J., Prandini, P., Brown, S.C., Torelli, S., Benson, M.A., Ponting, C.P., Estournet, B., Romero, N.B., Mercuri, E. *et al.* (2001) Mutations in the fukutin-related protein gene (FKRP) cause a form of congenital muscular dystrophy with secondary laminin alpha2 deficiency and abnormal glycosylation of alpha-dystroglycan. *Am. J. Hum. Genet.*, **69**, 1198–1209.
32. Grewal, P.K., Holzfeind, P.J., Bittner, R.E. and Hewitt, J.E. (2001) Mutant glycosyltransferase and altered glycosylation of alpha-dystroglycan in the myodystrophy mouse. *Nat. Genet.*, **28**, 151–154.
33. Manya, H., Chiba, A., Yoshida, A., Wang, X., Chiba, Y., Jigami, Y., Margolis, R.U. and Endo, T. (2004) Demonstration of mammalian protein O-mannosyltransferase activity: coexpression of POMT1 and POMT2 required for enzymatic activity. *Proc. Natl Acad. Sci. USA*, **101**, 500–505.
34. Lefeber, D.J., Schonberger, J., Morava, E., Guillard, M., Huyben, K.M., Verrijp, K., Grafakou, O., Evangeliou, A., Preijers, F.W., Manta, P. *et al.* (2009) Deficiency of Dol-P-Man synthase subunit DPM3 bridges the congenital disorders of glycosylation with the dystroglycanopathies. *Am. J. Hum. Genet.*, **85**, 76–86.
35. Stemple, D.L. (2004) TILLING—a high-throughput harvest for functional genomics. *Nat. Rev. Genet.*, **5**, 145–150.
36. Wienholds, E., van Eeden, F., Kosters, M., Mudde, J., Plasterk, R.H. and Cuppen, E. (2003) Efficient target-selected mutagenesis in zebrafish. *Genome Res.*, **13**, 2700–2707.
37. Bassett, D.I., Bryson-Richardson, R.J., Daggett, D.F., Gautier, P., Keenan, D.G. and Currie, P.D. (2003) Dystrophin is required for the formation of stable muscle attachments in the zebrafish embryo. *Development*, **130**, 5851–5860.
38. Hall, T.E., Bryson-Richardson, R.J., Berger, S., Jacoby, A.S., Cole, N.J., Hollway, G.E., Berger, J. and Currie, P.D. (2007) The zebrafish candyfloss mutant implicates extracellular matrix adhesion failure in laminin alpha2-deficient congenital muscular dystrophy. *Proc. Natl Acad. Sci. USA*, **104**, 7092–7097.
39. Parsons, M.J., Pollard, S.M., Saude, L., Feldman, B., Coutinho, P., Hirst, E.M. and Stemple, D.L. (2002) Zebrafish mutants identify an essential role for laminins in notochord formation. *Development*, **129**, 3137–3146.
40. Ervasti, J.M. and Campbell, K.P. (1993) A role for the dystrophin-glycoprotein complex as a transmembrane linker between laminin and actin. *J. Cell Biol.*, **122**, 809–823.
41. Coutinho, P., Parsons, M.J., Thomas, K.A., Hirst, E.M., Saude, L., Campos, I., Williams, P.H. and Stemple, D.L. (2004) Differential requirements for COPI transport during vertebrate early development. *Dev. Cell*, **7**, 547–558.
42. Hayashi, Y.K., Engvall, E., Arikawa-Hirasawa, E., Goto, K., Koga, R., Nonaka, I., Sugita, H. and Arahata, K. (1993) Abnormal localization of laminin subunits in muscular dystrophies. *J. Neurol. Sci.*, **119**, 53–64.
43. Schroder, M. and Kaufman, R.J. (2005) The mammalian unfolded protein response. *Annu. Rev. Biochem.*, **74**, 739–789.
44. Ron, D. and Walter, P. (2007) Signal integration in the endoplasmic reticulum unfolded protein response. *Nat. Rev.*, **8**, 519–529.
45. Brockington, M., Torelli, S., Prandini, P., Boito, C., Dolatshad, N.F., Longman, C., Brown, S.C. and Muntoni, F. (2005) Localization and functional analysis of the LARGE family of glycosyltransferases: significance for muscular dystrophy. *Hum. Mol. Genet.*, **14**, 657–665.
46. Fujimura, K., Sawaki, H., Sakai, T., Hiruma, T., Nakanishi, N., Sato, T., Ohkura, T. and Narimatsu, H. (2005) LARGE2 facilitates the maturation of alpha-dystroglycan more effectively than LARGE. *Biochem. Biophys. Res. Commun.*, **329**, 1162–1171.
47. Thornhill, P., Bassett, D., Lochmuller, H., Bushby, K. and Straub, V. (2008) Developmental defects in a zebrafish model for muscular dystrophies associated with the loss of fukutin-related protein (FKRP). *Brain*, **131**, 1551–1561.
48. Kawahara, G., Guyon, J.R., Nakamura, Y. and Kunkel, L.M. (2010) Zebrafish models for human FKRP muscular dystrophies. *Hum. Mol. Genet.*, **19**, 623–633.
49. Parsons, M.J., Campos, I., Hirst, E.M. and Stemple, D.L. (2002) Removal of dystroglycan causes severe muscular dystrophy in zebrafish embryos. *Development*, **129**, 3505–3512.
50. Cote, P.D., Moukhles, H., Lindenbaum, M. and Carbonetto, S. (1999) Chimaeric mice deficient in dystroglycans develop muscular dystrophy and have disrupted myoneural synapses. *Nat. Genet.*, **23**, 338–342.
51. Matsumura, K., Nonaka, I. and Campbell, K.P. (1993) Abnormal expression of dystrophin-associated proteins in Fukuyama-type congenital muscular dystrophy. *Lancet*, **341**, 521–522.
52. Arikawa, E., Ishihara, T., Nonaka, I., Sugita, H. and Arahata, K. (1991) Immunocytochemical analysis of dystrophin in congenital muscular dystrophy. *J. Neurol. Sci.*, **105**, 79–87.
53. Matsubara, S., Mizuno, Y., Kitaguchi, T., Isozaki, E., Miyamoto, K. and Hirai, S. (1999) Fukuyama-type congenital muscular dystrophy: close relation between changes in the muscle basal lamina and plasma membrane. *Neuromuscul. Disord.*, **9**, 388–398.
54. Nakano, I., Funahashi, M., Takada, K. and Toda, T. (1996) Are breaches in the glia limitans the primary cause of the micropolygyria in Fukuyama-type congenital muscular dystrophy (FCMD)? Pathological study of the cerebral cortex of an FCMD fetus. *Acta Neuropathol.*, **91**, 313–321.
55. Ishii, H., Hayashi, Y.K., Nonaka, I. and Arahata, K. (1997) Electron microscopic examination of basal lamina in Fukuyama congenital muscular dystrophy. *Neuromuscul. Disord.*, **7**, 191–197.
56. Beltran-Valero de Bernabe, D., Voit, T., Longman, C., Steinbrecher, A., Straub, V., Yuva, Y., Herrmann, R., Sperner, J., Korenke, C., Diesen, C. *et al.* (2004) Mutations in the FKRP gene can cause muscle-eye-brain disease and Walker-Warburg syndrome. *J. Med. Genet.*, **41**, e61.
57. Mercuri, E., Topaloglu, H., Brockington, M., Berardinelli, A., Pichiecchio, A., Santorelli, F., Rutherford, M., Talim, B., Ricci, E., Voit, T. *et al.* (2006) Spectrum of brain changes in patients with congenital muscular dystrophy and FKRP gene mutations. *Arch. Neurol.*, **63**, 251–257.
58. Takeda, S., Kondo, M., Sasaki, J., Kurahashi, H., Kano, H., Arai, K., Misaki, K., Fukui, T., Kobayashi, K., Tachikawa, M. *et al.* (2003) Fukutin is required for maintenance of muscle integrity, cortical histiogenesis and normal eye development. *Hum. Mol. Genet.*, **12**, 1449–1459.
59. Ackroyd, M.R., Skordis, L., Kaluarachchi, M., Godwin, J., Prior, S., Fidanboylu, M., Piercy, R.J., Muntoni, F. and Brown, S.C. (2009) Reduced expression of fukutin related protein in mice results in a model for fukutin related protein associated muscular dystrophies. *Brain*, **132**, 439–451.

60. Travers, K.J., Patil, C.K., Wodicka, L., Lockhart, D.J., Weissman, J.S. and Walter, P. (2000) Functional and genomic analyses reveal an essential coordination between the unfolded protein response and ER-associated degradation. *Cell*, **101**, 249–258.
61. Harding, H.P., Zhang, Y. and Ron, D. (1999) Protein translation and folding are coupled by an endoplasmic-reticulum-resident kinase. *Nature*, **397**, 271–274.
62. Bernales, S., McDonald, K.L. and Walter, P. (2006) Autophagy counterbalances endoplasmic reticulum expansion during the unfolded protein response. *PLoS Biol.*, **4**, e423.
63. Yorimitsu, T., Nair, U., Yang, Z. and Klionsky, D.J. (2006) Endoplasmic reticulum stress triggers autophagy. *J. Biol. Chem.*, **281**, 30299–30304.
64. Jimenez-Mallebrera, C., Torelli, S., Feng, L., Kim, J., Godfrey, C., Clement, E., Mein, R., Abbs, S., Brown, S.C., Campbell, K.P. *et al.* (2009) A comparative study of alpha-dystroglycan glycosylation in dystroglycanopathies suggests that the hypoglycosylation of alpha-dystroglycan does not consistently correlate with clinical severity. *Brain Pathol.*, **19**, 596–611.
65. MacLeod, H., Pytel, P., Wollmann, R., Chelmicka-Schorr, E., Silver, K., Anderson, R.B., Waggoner, D. and McNally, E.M. (2007) A novel FKRP mutation in congenital muscular dystrophy disrupts the dystrophin glycoprotein complex. *Neuromuscul. Disord.*, **17**, 285–289.
66. Senderek, J., Krieger, M., Stendel, C., Bergmann, C., Moser, M., Breitbach-Faller, N., Rudnik-Schoneborn, S., Blaschek, A., Wolf, N.I., Harting, I. *et al.* (2005) Mutations in SIL1 cause Marinesco-Sjogren syndrome, a cerebellar ataxia with cataract and myopathy. *Nat. Genet.*, **37**, 1312–1314.
67. Boito, C.A., Fanin, M., Gavassini, B.F., Cenacchi, G., Angelini, C. and Pegoraro, E. (2007) Biochemical and ultrastructural evidence of endoplasmic reticulum stress in LGMD2I. *Virchows Arch.*, **451**, 1047–1055.
68. Moore, C.J., Goh, H.T. and Hewitt, J.E. (2008) Genes required for functional glycosylation of dystroglycan are conserved in zebrafish. *Genomics*, **92**, 159–167.
69. Currie, P.D. and Ingham, P.W. (1996) Induction of a specific muscle cell type by a hedgehog-like protein in zebrafish. *Nature*, **382**, 452–455.
70. Thisse, C., Thisse, B., Schilling, T.F. and Postlethwait, J.H. (1993) Structure of the zebrafish snail1 gene and its expression in wild-type, spadetail and no tail mutant embryos. *Development*, **119**, 1203–1215.